

# OZONE STRUCTURE AND VARIABILITY IN THE UPPER TROPOSPHERE AND LOWER STRATOSPHERE AS SEEN BY ENVISAT AND ESA THIRD-PARTY MISSION LIMB PROFILING INSTRUMENTS

V.F. Sofieva<sup>(1)</sup>, J. Tamminen<sup>(1)</sup>, J. Hakkarainen<sup>(1)</sup>, E. Kyrölä<sup>(1)</sup>, M. Sofiev<sup>(1)</sup>, G. Stiller<sup>(2)</sup>, A. Laeng<sup>(2)</sup>, T. von Clarmann<sup>(2)</sup>, S. Lossov<sup>(2)</sup>, M. Weber<sup>(3)</sup>, N. Rappoe<sup>(3)</sup>, A. Rozanov<sup>(3)</sup>, D. Degenstein<sup>(4)</sup>, A. Bourassa<sup>(4)</sup>, K. A. Walker<sup>(5)</sup>, D. Hubert<sup>(6)</sup>, M. van Roozendaal<sup>(6)</sup>, C. Zehner<sup>(7)</sup>

<sup>(1)</sup>Finnish Meteorological Institute, P. O. Box 503, 00101 Helsinki, Finland, Email: viktoria.sofieva@fmi.fi

<sup>(2)</sup>Karlsruhe Institute of Technology, IMK, P.O. Box 3640, 76021 Karlsruhe, Germany

<sup>(3)</sup>Institute of Environmental Physics, Universitaet Bremen FB1, Otto-Hahn-Allee 1, D-28359 Bremen, Germany

<sup>(4)</sup>University of Saskatchewan, 116 Science Place, Saskatoon, SK S7N 5E2, Canada

<sup>(5)</sup>University of Toronto, Department of Physics, 60 St. George St., Toronto, Ontario, M5S 1A7, Canada

<sup>(6)</sup>Belgian Institute for Space Aeronomy (BIRA-IASB), Ringlaan 3, Brussels, Belgium

<sup>(7)</sup>ESA/ESRIN, Via Galileo Galilei CP. 64, 00044 Frascati (RM), Frascati, Italy

## ABSTRACT

In this technical note, we compare the spatio-temporal distributions and variations of the ozone field in the UTLS obtained from the limb instruments participating in the ESA Climate Change Initiative for Ozone (Ozone\_cci): MIPAS, SCIAMACHY and GOMOS on Envisat, OSIRIS on Odin, and ACE-FTS on SCISAT. We study seasonal variations and the influence of Asian Summer Monsoon on UTLS ozone.

The observational distributions by Ozone\_cci instruments are generally in good agreement. This consistency of the observed patterns allows creating Level 3 datasets and parameters, which can be useful for validation of chemistry climate models.

## 1. INTRODUCTION

Dynamical, chemical and radiative coupling between the stratosphere and troposphere are among the important processes that must be understood for prediction of global trends, including climate change [1]. Due to processes that result in variations of the tropopause height and temperature, and due to intensive stratosphere-troposphere exchange, ozone in the upper stratosphere and lower stratosphere (UTLS) is highly variable. Ozone abundances are dramatically different in the troposphere and in the stratosphere; therefore distribution of ozone can be indicative of different dynamical processes. From another point of view, ozone itself can affect the thermodynamic structure of the UTLS, as discussed e.g., in [2–4].

The UTLS region is difficult to explore from space. For limb-viewing satellite measurements, retrievals in the UTLS are challenging due to presence of clouds, lower signal-to-noise ratio and a strong gradient of species across the tropopause.

In this paper, we discuss the ozone distribution in the UTLS as observed by the limb profile instruments participating in the European Space Agency (ESA) Climate Change Initiative for ozone (Ozone\_cci). These are three instruments on board Envisat, GOMOS

(Global Ozone Monitoring by Occultation of Stars), MIPAS (Michelson Interferometer for Passive Atmospheric Sounding) and SCIAMACHY (SCanning Imaging Spectrometer for Atmospheric Chartography), as well as OSIRIS (Optical Spectrograph and InfraRed Imaging System) on Odin and ACE-FTS (Atmospheric Chemistry Experiment Fourier Transform Spectrometer) on SCISAT. The analyses are based on the ozone profile dataset included in the HARMonized dataset of OZone profiles (HARMOZ) [5]. All datasets have a sufficiently good resolution of 2–3 km in the UTLS. The information about processing versions of the datasets is collected in Table 1; for more information, see [5] and references therein.

Table 1. Processing versions of the ozone datasets used in the analyses

GOMOS	IPF V6 and FMI research processor
MIPAS	IMK research processor V5R_O3_220/221
SCIAMACHY	SCIAMACHY-IUP V2.9
OSIRIS	SaskMART v5.0x
ACE-FTS	V3.0

## 2. GENERAL CHARACTERIZATION OF OZONE PROFILES IN THE UTLS

The upper troposphere and the lower stratosphere are usually rather well covered by Ozone\_cci instruments. This is illustrated in Fig.1, which shows the mean and the standard deviation of the lowermost altitude of the ozone profiles for each instrument in 2007–2008. The lowest altitude usually depends on presence of clouds. For GOMOS, the lowest altitude depends also on star magnitude [6]. For bright stars, measurements go below the tropopause.

Fig. 2 illustrates the overall data consistency and typical uncertainty estimates. As observed in Fig. 2, the data from MIPAS, SCIAMACHY, OSIRIS and ACE-FTS are close to each other in the UTLS. GOMOS V6 data have a strong positive bias in the UTLS (black line), which was also reported in [7]. The development of the

advanced GOMOS processor optimized for the UTLS is ongoing [7]. The preliminary results show the new GOMOS ozone profiles are nearly unbiased with respect to other Ozone\_cci instruments in the tropical UTLS (black dashed line).

The uncertainties of ozone profiles in the UTLS are estimated to be a few tens of percent, as shown in Fig. 2 (right). Note that the SCIAMACHY uncertainty estimates are larger than those of other instruments, because they include also the smoothing error.

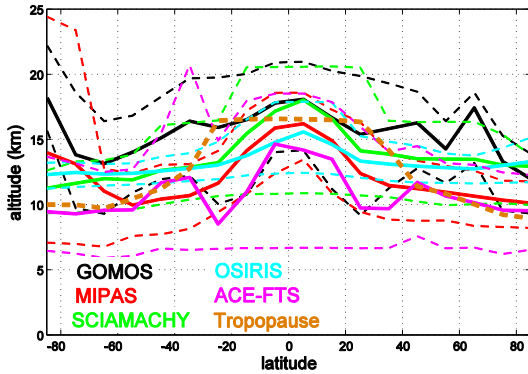


Figure 1. The mean (solid lines) and the standard deviation (dashed lines) of the lowermost altitudes for the five satellite instruments in 2007-2008. Brown dashed line represents the mean tropopause height.

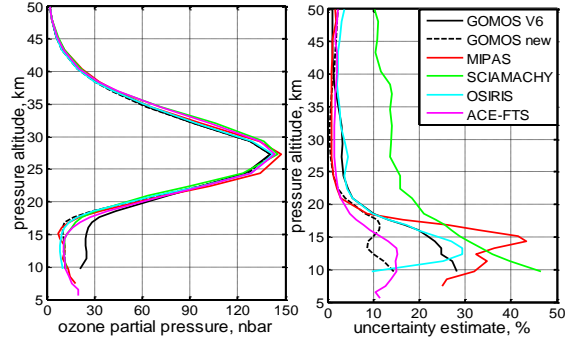


Figure 2. Left: mean ozone profiles from the Ozone\_cci instruments at latitudes 20°S–20°N in 2007–2008. Right: mean ozone uncertainty estimates for each instrument.

### 3. VALIDATION AGAINST GROUND-BASED MEASUREMENTS

In the Ozone\_cci project, an extensive validation of the ozone profiles from the limb instruments using collocated ozonesonde and lidar measurements has been performed. The details of the validation activity can be found in the Ozone\_cci Product Validation and Intercomparison Report (PVIR, [www.esa-ozone-cci.org/?q=webfm\\_send/148](http://www.esa-ozone-cci.org/?q=webfm_send/148)) and in [8]. For the analyses, satellite and ozonesonde data separated less than 500 km in space and less than 12 h in time have been selected. Ozonesonde data have been smoothed down to the vertical resolution of the satellite data.

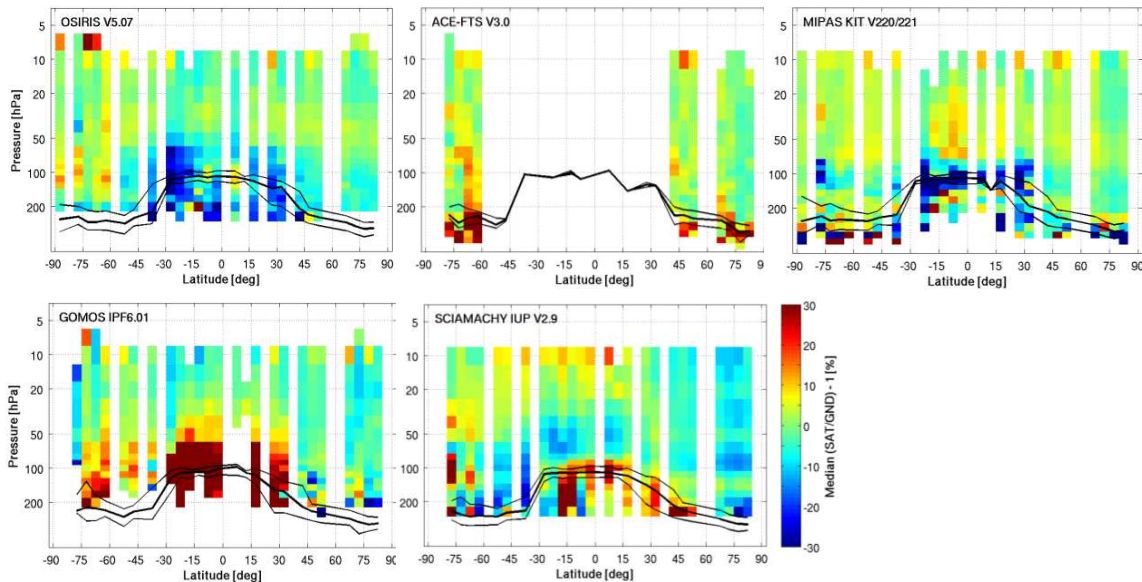


Figure 3. Median relative difference of satellite minus ground-based ozone profiles as a function of latitude. Solid black lines indicates the mean lapse-rate-tropopause pressure (thick lines) and its  $1\sigma$ -variations (thin lines), which are computed using sonde temperature profile.

The results of the comparison of the HARMOZ dataset with ozonesondes from NDACC, WOUDC and SHADOZ networks are summarized in Fig. 3. Usually, biases of the Ozone\_cci instruments with respect to ozonesondes are within  $\pm 20\%$ , with some instrument-specific features.

Large positive bias of GOMOS V6 profiles is clearly observed in Fig. 3. As discussed above, such a bias is not present in the advanced GOMOS retrievals [7].

Due to the low spatial sampling of the solar occultation instrument ACE-FTS, not all latitudes are covered with collocated ozonesonde data.

#### 4. GEOPHYSICAL PHENOMENA AS SEEN BY OZONE\_CCI INSTRUMENTS

In this section, we show how geophysical phenomena in the UTLS are represented by the Ozone\_cci data.

##### 4.1. Influence of Asian Summer Monsoon

The Asian Summer Monsoon (ASM) contains a strong anti-cyclonic vortex in the UTLS, spanning from Asia to the Middle East. The ASM has been recognized as a significant transport pathway for water vapor and pollutants to the stratosphere (e.g., [9,10]).

Still open questions related to the ASM influence include the structure of chemical composition and aerosols in the UTLS, water vapor budget and aerosol

cirrus cloud interaction, troposphere-stratosphere exchange, representation of the transport pathway in the chemistry-climate models, and long-term trends.

Fig.4 shows ozone distributions at 100 hPa in June-August from OSIRIS, ACE-FTS, MIPAS, and SCIAMACHY measurements. To obtain these maps, all available data have been used. The low ozone values in Asia associated with the strong upward motion of tropospheric air are clearly seen in these distributions, and peculiar features of ozone associated with the ASM are very similar in all datasets displayed.

Climate chemistry models capture the associated impact on ozone to some degree [10]. It should be noted that the UTLS region is challenging not only for satellite observations, but also for chemistry-transport models. Nowadays, there is a general tendency to extend the upper altitude limit in the models. Fig. 5 compares the ozone distributions at 100 hPa from MIPAS measurement with those simulated using the SILAM v. 5.5 chemistry-transport model [11]. SILAM is known as an air quality model, but now this model includes also the stratospheric chemistry and its upper altitudes extend up to the stratopause. As seen in Fig. 5, SILAM reproduces rather well the MIPAS distributions. As observed in both MIPAS and SILAM data, ozone in the ASM region is highly variable, even within one season. Intra-seasonal and inter-annual variations will be subject of future analyses.

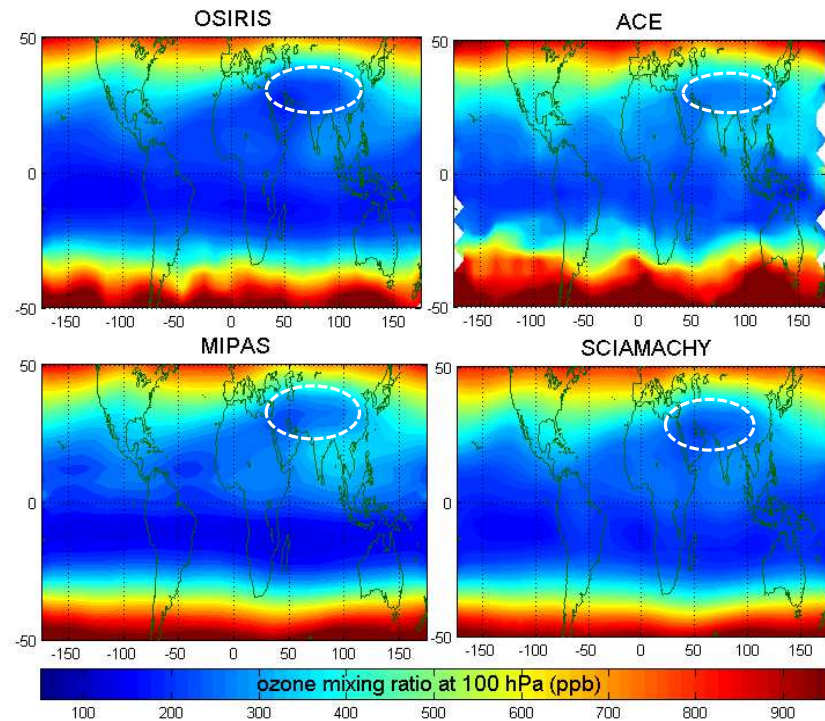


Figure 4. Mean ozone mixing ratio (ppb) at 100 hPa in the summer season (June-August), as inferred from all available measurements of the Ozone\_cci limb instruments. Ellipses indicate low ozone values associated with the Asian Summer Monsoon.

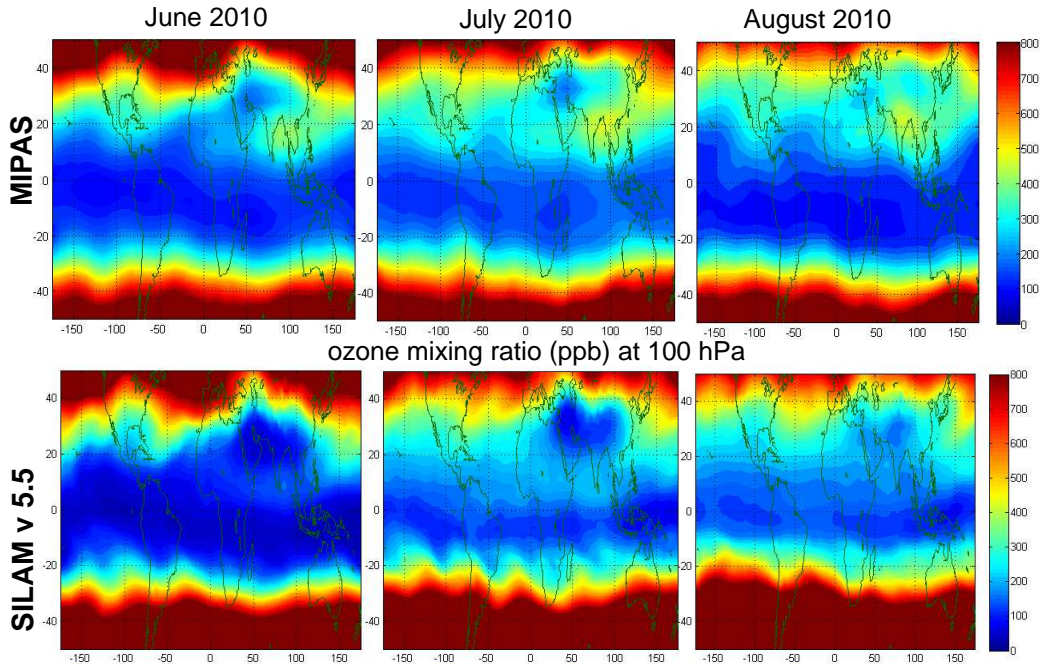


Figure 5. Ozone mixing ratio (ppb) in June (1<sup>st</sup> column), July (2<sup>nd</sup> column) and August 2010 (3<sup>rd</sup> column) from MIPAS measurements (top) and SILAM v.5.5 simulations (bottom).

#### 4.2. Seasonal cycle in the tropical UTLS

A pronounced annual cycle is observed in the tropics with approximately factor-of-two variations in the strength of upwelling and temperature variations of up to 8 K, with faster upwelling and colder temperatures during boreal winter (Fig. 6, top). The annual cycle is observed exclusively above ~15 km, which is roughly the bottom of the tropical tropopause layer [4,12].

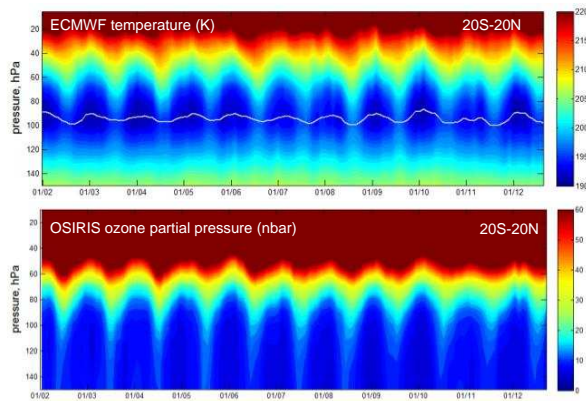


Figure 6. Time series of ECMWF temperature profiles (top) at 20°S–20°N and ozone partial pressure from OSIRIS (bottom). Gray line in the top panel indicates the mean tropopause pressure.

Originally, the tropical cycle was explained as a response to the annual cycle of the stratospheric

planetary wave forcing at high latitudes in winter-spring [13]. However, recent analyses indicate the important role of extra-tropical waves dissipating in subtropics and planetary waves generated within the tropics [4,14]. The tropical upwelling influences the vertical transport of trace constituents; this is especially important for ozone having a strong gradient across the tropical tropopause layer. The ozone annual cycle in the tropical UTLS is illustrated in Fig. 6 (bottom), which shows the zonally averaged ozone profiles from OSIRIS. A clear annual cycle is observed, with peculiar features, which are perfectly correlated with those of temperature. The ozone variations can be very useful for studying dynamical processes in the UTLS in connection with climate change [15].

The representation of the annual ozone cycle at 100 hPa is a standard test in climate model intercomparison [16]. Reproducing the tropical ozone annual cycle requires realistic model representation of dynamics and chemistry in both the troposphere and the stratosphere. As shown in [16] (the results of the comparison are reproduced in Fig.7, top), there is a large spread in the climate model simulations.

Fig. 7 (center) shows the tropical ozone seasonal cycle in the UTLS from the measurements by Ozone\_cci instruments. The seasonal cycle has been derived using all available data for OSIRIS, ACE-FTS, MIPAS and SCIAMACHY. For GOMOS, only the new retrieval data from year 2008 are shown.

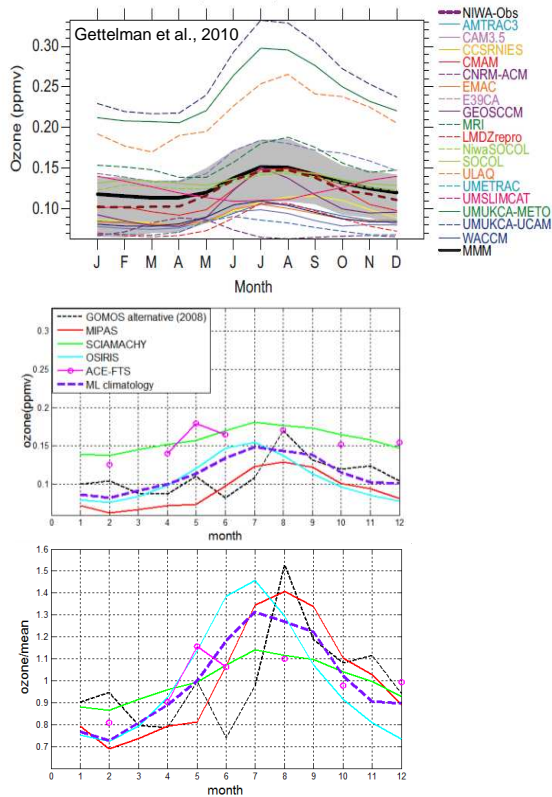


Figure 7. Top: from [16]: Annual cycle of tropical (20°S–20°N) 100 hPa ozone mixing ratio from various models and ozonesonde observations (NIWA dataset) for the period 1980–2005. Gray shaded region indicates 3 $\sigma$ -variability from NIWA observations (dashed brown line). For details of the models, see [16]. The multimodel mean (MMM) is the thick black line. Center: ozone mixing ratio at 100 hPa from Ozone\_cci instruments and ML ozone climatology [17] (dashed purple line). Bottom: amplitude of annual cycle at 100 hPa for Ozone\_cci instruments and ML climatology.

There are some biases between the Ozone\_cci instruments (Fig. 7, center), but they are much smaller than the spread of the climate models (Fig. 7, top). In Fig. 7 (center), the annual cycle from the McPeters&Labow ozone climatology (ML, [17]) is also shown. In this altitude region, the ML climatology is based on ozonesonde data. The annual cycle curves by ACE-FTS and GOMOS data have more fluctuations, as they are based on smaller samples. The amplitude of the annual cycle (i.e., monthly mean data divided by the annual mean) looks similar in most of the Ozone\_cci datasets. The amplitude of the annual cycle is smaller in SCIAMACHY data than in other observations. This is probably due to contamination with a priori information, which will be reduced in the next processing version [18]. Small differences in the phase of the annual cycle are, most probably, due to sampling patterns of different instruments.

### 4.3. Seasonal cycle in the extra-tropical UTLS

The seasonal cycle of ozone at 100 hPa in the extra-tropics is mainly driven by the Brewer-Dobson circulation, with maxima observed in spring (e.g., [19]). Fig. 8 shows the seasonal cycle at 40°N–60°N simulated by various climate-chemistry models (top) and observed by Ozone\_cci instruments (bottom). Climate models usually reproduce the extra-tropical annual cycle reasonably well, with some variations among the models. The observations of extra-tropical seasonal cycle by Ozone\_cci instruments at 100 hPa agree perfectly with each other and with the ML climatology (Fig. 8, bottom).

For the seasonal cycle in the Southern Hemisphere, a similar behavior is observed (Fig. 9).

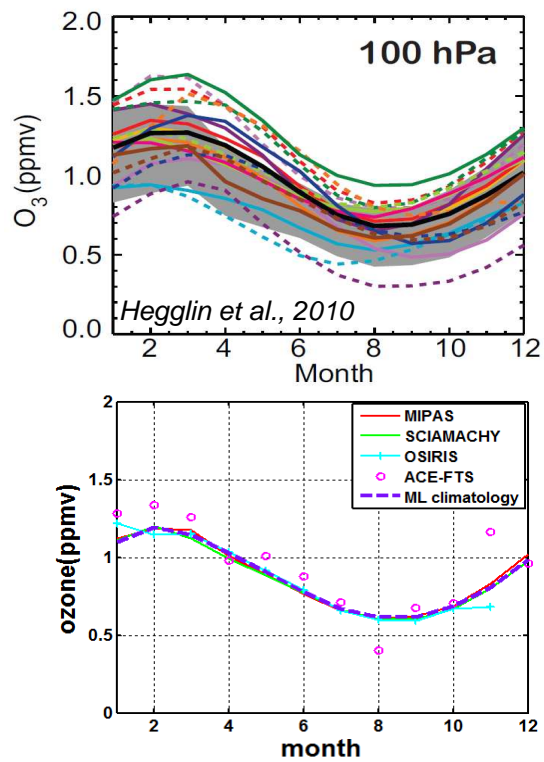


Figure 8. Top: from [19]: Annual cycle of 100 hPa ozone mixing ratio at 40°N–60°N from various for the period 1980–2005 (color lines). The multimodel mean is the thick black line. For details of the models, see [19]. Brown solid line is MIPAS measurements in 2005–2008 and the gray shaded region is the 1 $\sigma$ -variability of MIPAS observations. Bottom: ozone mixing ratio at 100 hPa from Ozone\_cci instruments and ML ozone climatology (dashed purple line).

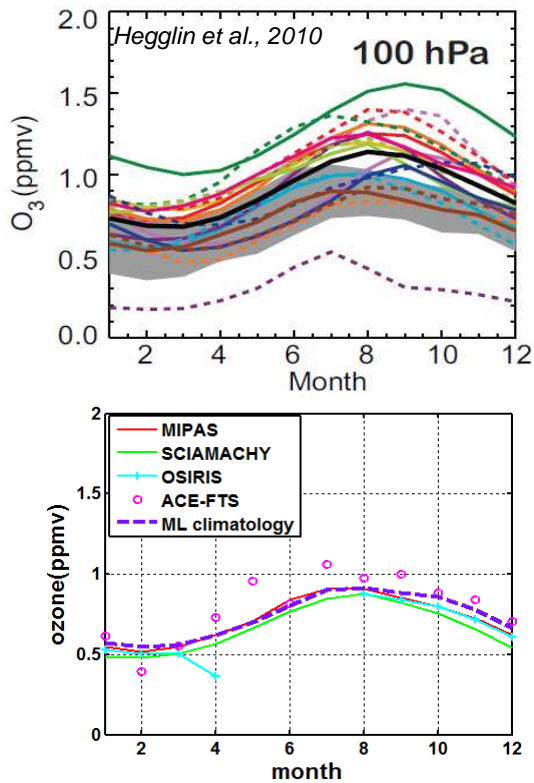


Figure 9. As Fig.8, but for latitudes 40°S–60°S.

## 5. SUMMARY AND DISCUSSION

Extensive validation and intercomparison of ozone limb profiles by the Ozone\_cci instruments has shown that the data in the UTLS are, in general, of good quality. Further data improvements are foreseen in upcoming processing versions.

The patterns of geophysical phenomena and variations observed by different instruments are in very good agreement thus providing useful information for testing chemistry-transport models.

The ozone profile data by Ozone\_cci instruments have been already used in UTLS related research. In particular, the ozone data have been used to study the influence of Indian Summer Monsoon [10], composition during the southern hemispheric biomass burning season in 2003 [20], jet characterization in the UTLS [21], low ozone events in the tropical upper troposphere [22] and the influence of Madden-Julian oscillation on ozone minimum over Tibetan plateau [23]. The ozone profiles from Ozone\_cci limb sensors have participated in the intercomparison of UTLS climatologies in the framework of the SPARC Data Initiative [24]. Recently, important analyses on ozone variability and trends in the tropical lower stratosphere have been performed [15,25].

In the framework of Ozone\_cci project, dedicated UTLS datasets will be created (both Level 2 and Level 3). The special focus will be on continuations of trend analyses

using Ozone\_cci limb profiles and creating climate data records.

## Acknowledgements

The work has been performed in the framework of the ESA Climate Change Initiative for ozone. The authors acknowledge the support of the European Space Agency (Ozone\_cci, ALGOM and DRAGON-3 projects), Canadian Space Agency, the Academy of Finland (projects ASTREX and INQUIRE). The Atmospheric Chemistry Experiment (ACE), also known as SCISAT, is a Canadian-led mission mainly supported by the Canadian Space Agency.

## 6. REFERENCES

1. Gettelman, A., Hoor, P., Pan, L. L., Randel, W. J., Hegglin, M. I. & Birner, T. 2011 The extratropical upper troposphere and lower stratosphere. *Rev. Geophys.* **49**, RG3003. (doi:10.1029/2011RG000355)
2. Fueglistaler, S., Haynes, P. H. & Forster, P. M. 2011 The annual cycle in lower stratospheric temperatures revisited. *Atmos. Chem. Phys.* **11**, 3701–3711. (doi:10.5194/acp-11-3701-2011)
3. Polvani, L. M. & Solomon, S. 2012 The signature of ozone depletion on tropical temperature trends, as revealed by their seasonal cycle in model integrations with single forcings. *J. Geophys. Res. Atmos.* **117**. (doi:10.1029/2012JD017719)
4. Randel, W. J. & Jensen, E. J. 2013 Physical processes in the tropical tropopause layer and their roles in a changing climate. *Nat. Geosci* **6**, 169–176.
5. Sofieva, V. F. et al. 2013 Harmonized dataset of ozone profiles from satellite limb and occultation measurements. *Earth Syst. Sci. Data* **5**, 349–363. (doi:10.5194/essd-5-349-2013)
6. Tamminen, J. et al. 2010 GOMOS data characterisation and error estimation. *Atmos. Chem. Phys.* **10**, 9505–9519. (doi:10.5194/acp-10-9505-2010)
7. Hakkarainen, J., Ialongo, I., Sofieva, V. F., Laine, M., Tamminen, J. & Kyrölä, E. 2015 Validation and alternative retrievals of GOMOS ozone profiles in the UTLS altitude region. In *Proceedings of the ATMOS conference, 8-12 June 2015, Heraklion, Greece*.
8. Hubert, D. et al. 2015 Ground-based assessment of the bias and long-term stability of fourteen

- limb and occultation ozone profile data. *Atmos. Meas. Tech. Discuss.*, submitted.
9. Park, M., Randel, W. J., Gettelman, A., Massie, S. T. & Jiang, J. H. 2007 Transport above the Asian summer monsoon anticyclone inferred from Aura Microwave Limb Sounder tracers. *J. Geophys. Res. Atmos.* **112**, D16309. (doi:10.1029/2006JD008294)
  10. Kunze, M. et al. 2010 Influences of the Indian Summer Monsoon on Water Vapor and Ozone Concentrations in the UTLS as Simulated by Chemistry–Climate Models. *J. Clim.* **23**, 3525–3544. (doi:10.1175/2010JCLI3280.1)
  11. Sofiev, M., Vira, J., Kouznetsov, R., Prank, M., Soares, J. & Genikhovich, E. 2015 Construction of an Eulerian atmospheric dispersion model based on the advection algorithm of M. Galperin: dynamic cores v.4 and 5 of SILAM v.5.5. *Geosci. Model Dev. Discuss.* **8**, 2905–2947. (doi:10.5194/gmdd-8-2905-2015)
  12. Fueglistaler, S., Dessler, A. E., Dunkerton, T. J., Folkins, I., Fu, Q. & Mote, P. W. 2009 Tropical tropopause layer. *Rev. Geophys.* **47**. (doi:10.1029/2008RG000267)
  13. Holton, J. R., Haynes, P. H., McIntyre, M. E., Douglass, A. R., Rood, R. B. & Pfister, L. 1995 Stratosphere-troposphere exchange. *Rev. Geophys.* **33**, 403–439.
  14. Chen, G. & Sun, L. 2011 Mechanisms of the Tropical Upwelling Branch of the Brewer–Dobson Circulation: The Role of Extratropical Waves. *J. Atmos. Sci.* **68**, 2878–2892. (doi:10.1175/JAS-D-11-044.1)
  15. Aschmann, J., Burrows, J. P., Gebhardt, C., Rozanov, A., Hommel, R., Weber, M. & Thompson, A. M. 2014 On the hiatus in the acceleration of tropical upwelling since the beginning of the 21st century. *Atmos. Chem. Phys.* **14**, 12803–12814. (doi:10.5194/acp-14-12803-2014)
  16. Gettelman, A. et al. 2010 Multimodel assessment of the upper troposphere and lower stratosphere: Tropics and global trends. *J. Geophys. Res. Atmos.* **115**. (doi:10.1029/2009JD013638)
  17. McPeters, R. D. & Labow, G. J. 2012 Climatology 2011: An MLS and sonde derived ozone climatology for satellite retrieval algorithms. *J. Geophys. Res.* **117**, D10303. (doi:10.1029/2011JD017006)
  18. Jia, J., Rozanov, A., Ladstätter-Weissenmayer, A. & P. Burrows, J. 2015 Global validation of improved SCIAMACHY scientific ozone limb data using ozonesonde measurements. *Atmos. Meas. Tech. Discuss.* **8**, 4817–4858. (doi:10.5194/amtd-8-4817-2015)
  19. Hegglin, M. I. et al. 2010 Multimodel assessment of the upper troposphere and lower stratosphere: Extratropics. *J. Geophys. Res. Atmos.* **115**. (doi:10.1029/2010JD013884)
  20. Von Clarmann, T. et al. 2007 MIPAS measurements of upper tropospheric C<sub>2</sub>H<sub>6</sub> and O<sub>3</sub> during the southern hemispheric biomass burning season in 2003. *Atmos. Chem. Phys.* **7**, 5861–5872. (doi:10.5194/acp-7-5861-2007)
  21. Manney, G. L. et al. 2011 Jet characterization in the upper troposphere/lower stratosphere (UTLS): applications to climatology and transport studies. *Atmos. Chem. Phys.* **11**, 6115–6137. (doi:10.5194/acp-11-6115-2011)
  22. Cooper, M. J., Martin, R. V., Livesey, N. J., Degenstein, D. A. & Walker, K. A. 2013 Analysis of satellite remote sensing observations of low ozone events in the tropical upper troposphere and links with convection. *Geophys. Res. Lett.* **40**, 3761–3765. (doi:10.1002/grl.50717)
  23. Liu, C., Liu, Y., Cai, Z., Gao, S., Lü, D. & Kyrölä, E. 2009 A Madden–Julian Oscillation-triggered record ozone minimum over the Tibetan Plateau in December 2003 and its association with stratospheric ‘low-ozone pockets’. *Geophys. Res. Lett.* **36**. (doi:10.1029/2009GL039025)
  24. Neu, J. L. et al. 2014 The SPARC Data Initiative: Comparison of upper troposphere/lower stratosphere ozone climatologies from limb-viewing instruments and the nadir-viewing Tropospheric Emission Spectrometer. *J. Geophys. Res. Atmos.* **119**, 6971–6990. (doi:10.1002/2013JD020822)
  25. Sioris, C. E., McLinden, C. A., Fioletov, V. E., Adams, C., Zawodny, J. M., Bourassa, A. E., Roth, C. Z. & Degenstein, D. A. 2014 Trend and variability in ozone in the tropical lower stratosphere over 2.5 solar cycles observed by SAGE II and OSIRIS. *Atmos. Chem. Phys.* **14**, 3479–3496. (doi:10.5194/acp-14-3479-2014)